CO2-responsive CCT protein interacts with 14-3-3 proteins and controls the expression of starch synthesis-related genes

Fukayama, Hiroshi ; Miyagawa, Fumihiro ; Shibatani, Naoki ; Koudou, Aiko ; Sasayama, Daisuke ; Hatanaka, Tomoko ; Azuma, Tetsushi ;…

(Citation)
Plant, Cell & Environment,44(8):2480-2493

(Issue Date)
2021-08

(Resource Type)
journal article

(Version)
Accepted Manuscript

CO_2-Responsive CCT Protein interacts with 14-3-3 proteins and controls the expression of starch synthesis-related genes

Hiroshi Fukayama[1], Fumihiro Miyagawa[1], Naoki Shibatani[1], Aiko Koudou[1], Daisuke Sasayama[2], Tomoko Hatanaka[2], Tetsushi Azuma[1], Yasuo Yamauchi[3], Daisuke Matsuoka[4], Ryutaro Morita[1]

[1]Laboratory of Tropical Plant Science, Graduate School of Agricultural Science, Kobe University, Kobe, 657-8501 Japan

[2]Laboratory of Crop Science, Graduate School of Agricultural Science, Kobe University, Kobe, 657-8501 Japan

[3]Laboratory of Functional Phytochemistry, Graduate School of Agricultural Science, Kobe University, Kobe, 657-8501 Japan

[4]Biosignal Research Center, Kobe University, 1-1 Rokkodai-cho, Nada-ku, Kobe 657-8501 Japan

Running Head: CRCT interacts with 14-3-3 proteins

Correspondence:

Hiroshi Fukayama, PhD

Laboratory of Tropical Plant Science, Graduate School of Agricultural Science,

Kobe University, Kobe, 657-8501 Japan

E-mail: fukayama@people.kobe-u.ac.jp

Present address:

Daisuke Matsuoka, Division of Food Design, Faculty of Nutrition, Koshien University, Takarazuka, 665-0006 Japan

Ryutaro Morita, Laboratory of Crop Science, Graduate School of Agricultural and Life Sciences, The University of Tokyo, Tokyo, 113-8657 Japan

Funding information

This work was supported by This work was supported by Japan Society for the Promotion of Science KAKENHI (22114511) and Hyogo Science and Technology Association (31071).

Abstract

CO_2 responsive CCT protein (CRCT) is a positive regulator of starch synthesis related genes such as *ADP-glucose pyrophosphorylase large subunit 1* and *starch branching enzyme I* particularly in the leaf sheath of rice (*Oryza sativa* L.). The promoter *GUS* analysis revealed that *CRCT* expressed exclusively in the vascular bundle, whereas starch synthesis related genes were expressed in different sites such as mesophyll cell and starch storage parenchyma cell. However, the chromatin immunoprecipitation (ChIP) using a FLAG-CRCT overexpression line and subsequent qPCR analyses showed that the 5'-flanking regions of these starch synthesis-related genes tended to be enriched by ChIP, suggesting that CRCT can bind to the promoter regions of these genes. The monomer of CRCT is 34.2 kDa, however CRCT was detected at 270 kDa via gel filtration chromatography, suggesting that CRCT forms a complex *in vivo*. Immunoprecipitation and subsequent MS analysis pulled down several 14-3-3-like proteins. A yeast two-hybrid analysis and bimolecular fluorescence complementation assays confirmed the interaction between CRCT and 14-3-3-like proteins. Although there is an inconsistency in the place of expression, this study provide important findings regarding the molecular function of CRCT to control the expression of key starch synthesis-related genes.

KEYWORDS

CO_2 response, CCT protein, 14-3-3 protein, protein interaction, Starch synthesis, transcription

1. INTRODUCTION

Starch is a major photosynthetic product and is highly accumulated as a storage polysaccharide in the reproductive organs of plants such as seeds and tubers. In addition, the starch is utilized for transient carbon storage of photosynthate in vegetative organs, i.e., leaf for most plants as well as leaf sheath for some gramineous plants, including rice. Rice is an important food crop and a model plant for the genomic analysis of monocots. In rice, starch is highly accumulated in the leaf sheath during the vegetative stage and remobilized to the reproductive organs at the grain-filling stage. This carbon remobilization accounted for no less than 30% of grain carbon (Cook & Yoshida, 1972), which can be particularly important for securing yield under limited solar radiation during the grain-filling stage (Okamura et al., 2013). A greater capacity of starch accumulation in the leaf sheath can reduce the occurrence of chalky grains under elevated temperature (Morita & Nakano, 2011). Thus, the capacity of starch accumulation in the vegetative organ is an important determinant of rice yield and quality.

Starch synthesis is a complex biochemical reaction catalyzed by multiple enzymes such as ADP-glucose pyrophosphorylase (AGPase), starch synthase, granule-bound starch synthase, α-glucan phosphorylase (Pho), starch branching enzyme (BE) and starch debranching enzyme. It is well known that the starch level increases markedly in vegetative organs of plants when grown under elevated CO_2 conditions (Ainsworth, & Long, 2005). Previously, we screened CO_2-responsive genes by microarray and identified a gene encoding a novel CONSTANS, CONSTANS-Like and TOC1 (CCT) domain-containing protein, designated *CO_2-responsive CCT protein* (*CRCT*), in rice (Fukayama et al., 2009; Morita et al., 2015). The starch content in the leaf sheath was greatly increased in *CRCT* overexpression lines and decreased in *CRCT* knockdown lines (Morita et al., 2015). The expression of multiple genes related to starch synthesis such as *AGPase large subunit 1* (*OsAGPL1*) and *BE I* (*OsBEI*) were highly correlated with the expression levels of *CRCT* in those transgenic rice lines, suggesting that *CRCT* is a positive regulator of starch accumulation in vegetative tissues. In addition, the increase in capacity of starch accumulation in vegetative organs by *CRCT* overexpression led to the

enhancement of photosynthetic capacity of rice when grown under elevated CO_2 condition (Morita et al., 2016). Moreover, analysis of the chain-length distribution of starch showed that the level of short chains with a degree of polymerization from 5 to 14 was positively correlated with the expression level of *CRCT* (Morita et al., 2019). These results suggest that *CRCT* can control the structure as well as the quantity of starch in the vegetative organs.

CRCT contains a CCT domain. In plants, CCT domain-containing proteins are mostly involved in the processes of photoperiodic flowering or circadian rhythms (Valverde, 2011; Li, & Xu, 2017). CCT domain-containing proteins are divided into three groups: the CONSTANS-like (COL) family with one or two zinc-finger B-box domains, the pseudo-response regulator family with a pseudo receiver domain and the CCT motif family with no such additional conserved domains (Cockram et al., 2012). *CRCT* belongs to the CCT motif family (Morita et al., 2015), and this family is thought to have evolved from a common ancestor *COL* gene and lost its B-box domains (Cockram et al., 2012). Although there have been no reports of functional analysis of *CRCT* orthologue in other plants, CCT motif family members are known to have diverse physiological functions in plants. For example, *Grain number, plant height, and heading date 7* (*Ghd7*) is a pleiotropic gene that controls the plant height, chlorophyll content, and yield, as well as the heading date in rice (Xue et al., 2008; Wang et al., 2015). *ZmCCT* was reported to be a major determinant of tassel size in maize (Xu et al., 2017). *ASML2* in *Arabidopsis thaliana* responds to sugar level and regulates some carbon metabolism-related genes (Masaki et al., 2005). Considering these functions, CCT motif family genes may play an important role in determining the plant growth and yield in plants.

The CCT domain has a nuclear localization signal (NLS) and thus is responsible for nuclear localization of proteins with this domain (Robson et al., 2001). More importantly, the CCT domains of CONSTANS and TOC1 were found to bind directly to DNA with CORE elements (Tiwari et al., 2010; Gendron et al., 2012). In addition, CONSTANS physically interacts with Nuclear Factor-Y transcription factors (NF-YB and NF-YC) to bind CORE elements in *Arabidopsis* (Gnesutta et al., 2017). Heading date 1, an orthologue of CONSTANS in rice, interacts with Ghd7 and binds to the promoter of a key flowering inducer, Early heading date 1

(Nemoto et al., 2016). The founding member of a PRR family CCT protein, TOC1 can interact with the F-box protein ZEITLUPE to control the circadian clock genes (Fujiwara et al., 2008). Thus, these representative CCT proteins function by interacting with other proteins.

CRCT can be described as a positive regulator of starch synthesis but the molecular function of this protein has been largely unknown. In this study, we carried out chromatin immunoprecipitation (ChIP) assays and showed that CRCT can bind to the promoter region of starch synthesis related gens. In addition, we used immunoprecipitation to identify 14-3-3 proteins associated with CRCT. This interaction was confirmed by yeast two-hybrid analysis and bimolecular fluorescence complementation (BiFC) assays. These findings gave us clues to a possible mechanism of how CRCT controls starch synthesis in vegetative organs.

2. MATERIALS AND METHODS

2.1 Plant Growth Conditions

Non-transgenic rice (*Oryza sativa* L. cv. Nipponbare), CRCT overexpression line (driven by Actin promoter; Morita et al. 2015), FLAG-CRCT overexpression line, and CRCT knockout line were grown in paddy soil under natural light conditions in a temperature-controlled greenhouse (30°C day/25°C night). Rice seedlings at the 4.5 leaf stage were transplanted into 1 L pots supplemented with 2.0 g chemical fertilizer (N:P:K=8:8:8), 0.5 g slow-release fertilizer, 0.15 g micronutrient, and 1.5 g silicate fertilizer. For qRT-PCR and starch content analyses, the seedlings of six rice cultivars (Nipponbare, Koshihikari, Habataki, Takanari, Momiroman, Leafstar) were transplanted into 1/5000 Wagner pots supplemented with 0.6 g N chemical fertilizer, 1.0 g slow-release fertilizer, 0.4 g micronutrient, and 4.0 g silicate fertilizer per pot. These plants were grown under natural light and temperature in a net house. The leaf blade and leaf sheath were sampled at 18:00-19:00 (photoperiod of 5:00-19:00) on sunny days, immediately frozen in liquid nitrogen and stored at -80°C until required.

2.2 qRT-PCR Analyses

Total RNA was isolated from rice tissues using an RNeasy Plant Mini Kit (Qiagen, http://www.qiagen.com) according to the manufacturer's instructions. The first strand cDNA was synthesized from total RNA with an oligo $(dT)_{18}$ and a random hexamer as primers using PrimeScript II 1st Strand cDNA Synthesis Kit (Takara, http://www.takara-bio.co.jp). The qRT-PCR was performed using gene-specific primers (Table S1), TBgreen Premix Ex Tag GC (Takara) and a thermal cycler (MyGoPro, IT-IS Life Science Ltd., http://www.itislifescience.com). Expression of the *Actin* was examined as an internal control.

2.3 Determination of Starch Content

The 8th leaf sheath at the 9.5 leaf stage was sampled in the early evening. The starch content was determined by a coupled enzyme assay using an ENZYTEC Starch kit (Code No. E1268, r-biopharm, http://www.r-biopharm.com/) as described previously (Morita et al., 2015).

2.4 Vector Construction and Transformation of Rice

Rice genomic DNA was prepared from young fully expanded leaves using cetyltrimethylammonium bromide as described previously (Morita, Hatanak, Misoo, & Fukayama, 2014). To construct the promoter::*GUS* chimeric gene, 5'-flanking region including 5'-UTR and partial coding region of *glucose 6-phosphate/phosphate translocator 2* (*OsGPT2*; -2428 to +654, numbered from the translation initiation site), *OsAGPL1* (-3758 to +200), *AGPase small subunit 1* (*OsAGPS1*; -1943 to +851), *OsBE1* (-2049 to +263) and *Pho1* (*OsPho1*; -2037 to +1431) were amplified by PCR using gene specific primers (Table S1). The amplified DNAs were fused upstream of *GUS* into a binary vector pBI-Hm.

For overexpression of FLAG-CRCT, the 3xFLAG fragment was amplified by PCR using the primers shown in Table S1 and the p3XFLAG-CMV plasmid (Sigma-Aldrich, https://www.sigmaaldrich.com) as a template. The obtained 3xFLAG fragment was fused to the

rice *Actin* promoter and cloned into a binary vector pBI-Hm. First-strand cDNA was synthesized from total RNA with an oligo $(dT)_{18}$ primer using PrimeScript II first-strand cDNA synthesis kit (Takara) as above. The coding region of *CRCT* was amplified by RT-PCR using gene specific primers (Table S1) and fused downstream of 3xFLAG into pBI-Hm.

The plasmid construction for the CRCT knockout by CRISPR/Cas9 was carried out according to Mikami, Toki, & Endo, (2015). A target sequence created from two primers (Table S1) was cloned into the vector pZK_OsU6-gRNA. The connected DNA fragment of *OsU6* promoter, target sequence, sgRNA scaffold and poly(T) was obtained from the digestion of the vector by *I-SceI* and inserted into *I-SceI* site of binary vector pZH_MMCas9.

These constructs were introduced into rice via *Agrobacterium*-mediated gene transfer. Antibiotic-resistant transgenic rice plants were regenerated and grown in soil as stated above.

2.5 Histochemical Analysis

Histochemical analysis of GUS activity was basically performed as described (Matsuoka, & Numazawa, 1991). Rice tissues were incubated in 90% (v/v) acetone for 30 min and washed three times with PBS. Then, these samples were incubated in the GUS staining solution (50 mM potassium phosphate, 5 mM potassium ferricyanide, 5 mM potassium ferrocyanide, 2 mM 5-bromo-4-chloro-3-indoyl-β-D-glucuronic acid and 0.1% (v/v) Triton X-100) for 3 to 48 h at 37°C. An ethanol wash was performed to stop the GUS reaction and remove chlorophyll from the tissues. These tissues were observed by light microscope or stereoscopic microscope.

2.6 SDS-PAGE and western blotting

Rice tissues were ground into a fine powder in liquid nitrogen using a mortar and pestle. The proteins were then extracted by suspending the powder in extraction buffer A (50 mM Tris-HCl, 1 M hexylene glycol, 10 mM $MgCl_2$, 10 mM 2-mercaptoethanol, 0.01 mM leupeptin, 1 mM polyvinylpolypyrrolidone, and 1× EDTA-Free Complete Protease Inhibitor Cocktail (Roche,

https://www.roche-diagnostics.jp), pH 9.0). The homogenate was centrifuged at 15,000 × g for 5 min at 4°C, and the supernatants were collected.

The soluble proteins were separated by SDS-PAGE (12%) and subjected to Coomassie Blue staining, silver staining using Silver Stain MS Kit (Fujifilm Wako Chemical, https://labchem-wako.fujifilm.com/jp), or western blotting using anti-CRCT (Morita et al., 2019) or anti-DYKDDDDK (FLAG) tag monoclonal antibodies (Fujifilm Wako Chemical). Immunoreacted bands were visualized with the ECL Select Western Blotting Detection Kit (GE Healthcare, http://www3.gehealthcare.co.jp) and exposed to X-ray film as described previously (Masumoto et al., 2011).

2.7 ChIP analysis

ChIP experiments were performed as described by Buzas et al. (2011). The non-crosslinked leaf sheath of the CRCT-FLAG overexpression line was used for this experiment. FLAG-CRCT associated DNA was immunoprecipitated using anti-DYKDDDDK tag antibody beads (Fujifilm Wako Chemical). Immunoprecipitated DNAs and input DNAs were purified using QIAquick PCR Purification Kit (Qiagen). ChIP-qPCR was performed using gene-specific primers (Table S1). Purified immunoprecipitated DNAs and input DNAs were used as templates, and qPCR was carried out using TBgreen Premix Ex Tag GC (Takara) and a thermal cycler (MyGoPro, IT-IS Life Science Ltd.) according to the manufacturer's instructions. The 18S ribosomal RNA gene (XR_003238822) was examined as a reference.

2.8 Gel filtration chromatography

The soluble proteins of the CRCT overexpression line in the crude extract with buffer A (100 μL) were separated by gel filtration chromatography using the SMART system (GE Healthcare) with a Superose 12 PC3.2/30 column equilibrated with buffer A containing 100 mM NaCl. Separation was performed at a flow rate of 40 μL min^{-1}. Fractions (40 μL) were collected and

subjected to western blot analysis.

2.9 Immunoprecipitation

The crude extracts (with buffer A) of the leaf sheath of the FLAG-CRCT overexpression line and CRCT knock out line were incubated with anti-DYKDDDDK tag antibody beads (Fujifilm Wako Chemical) at 4˚C for 1 h. After incubation, the beads were collected using a magnet and washed three times with a washing buffer (20 mM Tris-HCl pH 7.4, 200 mM NaCl, 2.5 mM MgCl2, 0.05% (w/v) NP-40). FLAG-CRCT associated proteins were eluted by incubating the beads with 500 μg mL^{-1} DYKDDDDK peptide (Fujifilm Wako Chemical) in 10 mM Tris-HCl pH 7.4, 150 mM NaCl at 4˚C for 30 min. The eluted proteins were then subjected to SDS-PAGE and identified by LC-MS analysis.

2.10 Yeast two-hybrid analysis and transcription activation activity

A yeast two-hybrid assay was performed using a HybriZAP-2.1 two-hybrid vector system (Stratagene, https://www.agilent.com/) as described previously (Matsuoka, Yasufuku, Furuya, & Manmori, 2015). The full-length coding regions of *CRCT*, *GF14A* and *GF14B* were amplified by RT-PCR using gene-specific primers (Table S1). The PCR product of *CRCT* was cloned into the pAD-GAL4-2.1 vector for the expression of GAL4 transcriptional activation domain fusion proteins. The PCR products of *GF14A* and *GF14B* were inserted into the pBD-GAL4 Cam vector for the expression of GAL4 DNA-binding domain fusion proteins. Each pair of bait and prey vectors was cotransformed into yeast (strain YRG-2). The transformation was confirmed by growth on the synthetic media plate lacking Leu and Trp (SD^{2-}). The protein interaction was monitored by growth on the synthetic media plate lacking Leu, Trp and His (SD^{3-}).

Transcriptional activation activity was analyzed using the two-hybrid vector system without pAD-GAL4-2.1 vector. Eight different *CRCT* fragments were amplified by PCR using primers listed in Table S1 and cloned into the pBD-GAL4 Cam vector. The vectors were transformed

into the yeast. The transformation and transcription activation activity were monitored by growth of yeast on the synthetic media plate lacking Trp (SD^{1-}) and Trp and His (SD^{2-}), respectively.

2.11 Subcellular localization analysis using GFP and BiFC assay

The cDNA sequences containing the full length coding region of *CRCT* (amino acid 1-308) and the CCT domain (amino acid 235-308) were amplified by RT-PCR using gene specific primer pairs (Table S1). The amplified cDNAs were each cloned into a GFP expression vector pHTII-CaMV35S-sGFP(S65T)-nos (Chiu et al., 1996). The GFP expression vectors were introduced into the epidermis of onion (*Allium cepa*) by particle bombardment using 1-μm gold particles and a gene delivery system (PDS-1000, Bio-Rad, https://www.bio-rad.com). After a 24 h incubation in the dark at room temperature, the epidermis was peeled from the bombarded segment, and the fluorescence from GFP and DAPI were observed with a fluorescence microscope (ECLIPSE 80i, Nikon, https://www.nikon.co.jp) through FITC and V-2A cubes, respectively.

A BiFC experiment was carried out as described in Kodama, & Wada, (2009), except superfolder GFP (sfGFP) was used in this experiment (Fujii and Kodama, 2015). The full length coding regions of *CRCT* and *GF14A* were amplified by RT-PCR using gene-specific primers (Table S1). The PCR fragments were inserted into the pBsfGN155-MXMT vector containing the N-terminal region of sfGFP (sfGN) with 7-methylxanthine methyltransferase from *Coffea arabica* (MXMT) and the pBsfGC155-MXMT vector with the C-terminal region of sfGFP with MXMT by replacing MXMT (pBsfGN155-MXMT and pBsfGC155-MXMT were generous gifts from Dr. Kodama and used as a arbitrary control for BiFC in this study). Appropriate combinations of BiFC expression vectors were introduced into the epidermis of onion (*Allium cepa*) as described above. As a control for transformation, a vector containing CaMV35S::DsRed (pHTII-CaMV35S-DsRed) was introduced together with the BiFC expression vectors. The fluorescence from sfGFP, DsRed and DAPI were observed with a

fluorescence microscope (ECLIPSE 80i, Nikon) through FITC, G-2A and V-2A cubes, respectively.

2.12 Accession numbers

Gene sequence data can be found at the Rice Annotation Project Database (RAP-DB) under RAP-ID of *CRCT* (Os05g0595300), *GF14A* (Os08g0480800), *GF14B* (Os04g0462500), *OsGPT2* (Os07g0523600), *OsAGPL1* (Os05g0580000), *OsAGPS1* (Os09g0298200), *OsBEI* (Os06g0726400) and *OsPho1* (Os03g0758100). The sequences of 5'-flanking region can be found at the Genbank under the accession numbers of *OsGPT2* (AP003827), *OsAGPL1* (AC007858), *OsAGPS1* (AP004011), *OsBEI* (AP004685) and *OsPho1* (AC079887). *Actin* can be found at the Genbank under the accession numbers of AB047313.

3. RESULTS

3.1 Expression of starch synthesis-related genes

In our previous study, the expressions of starch synthesis-related genes such as *OsGPT2*, *OsAGPL1*, *OsAGPS1*, *OsBEI* and *OsPho1* were highly correlated with the expression of *CRCT* in the leaf sheath of *CRCT* overexpression lines and knockdown lines (Morita et al., 2015; Morita et al., 2019). There are considerable differences in the starch content in the leaf sheath among rice varieties (Goda et al., 2016). Thus, in this study, the relationships between the expression levels of *CRCT* and the starch synthesis-related genes were analyzed in the six rice cultivars, Nipponbare, Koshihikari, Habataki, Takanari, Momiroman and Leafstar (Figure 1). Among these cultivars, Nipponbare was used for the production of transgenic lines. Koshihikari is the most popular cultivar in Japan. Habataki, Takanari and Momiroman are representative high-yielding varieties. However, the pattern of changes in the nonstructural carbohydrate (mainly starch) content in the leaf sheath and culm during the reproductive stage were different

between Takanari and Momiroman (Yoshinaga et al., 2013). For example, the content of nonstructural carbohydrate in the leaf sheath and culm were significantly lower in Takanari than in Momiroman at the grain-filling stage. Leafstar is characterized as lodging resistant and has a high starch content in straw (Ookawa et al., 2010). Using the leaf sheath of these cultivars, the expression levels of *CRCT* were compared with the expression levels of starch synthesis-related genes by qRT-PCR. The expression levels of *OsAGPL1*, *OsAGPS1* and *OsPho1* highly correlated with that of CRCT. In contrast, weak or no correlation with CRCT expression were observed in *OsGPT2* and *OsBEI*. However, when limited to Nipponbare, Koshihikari and Takanari, the *OsBEI* expression was correlated with the *CRCT* expression. While not apply to all, the expression level of *CRCT* can be a major determinant of natural variation in the expression level of multiple starch synthesis-related genes.

The relationship between the expression level of *CRCT* and starch content was also analyzed using these cultivars. In our previous study, it was clearly shown that starch content was greatly increased in the *CRCT* overexpression lines and decreased in the *CRCT* knockdown lines (Morita et al., 2015). However, a significant correlation was not observed between the starch content and the expression levels of *CRCT* in the leaf sheath among these rice cultivars (Figure 1). This tendency was the same even when limited to the cultivars showing the correlation between the *OsBEI* expression and the *CRCT* expression.

3.2 Tissue and cellular specificity of starch synthesis-related gene expression

Tissue and cellular specificity of starch synthesis-related gene expression was studied by histochemical staining of GUS activity in transgenic rice with the promoter::*GUS* chimeric genes. As reported previously (Morita et al., 2015), *CRCT* expression in the leaf blade and leaf sheath was mostly found in vascular bundles, particularly around the phloem (Figure 2a, g). This pattern of expression was not affected by the extension of staining time or sucrose treatment to increase sensitivity of detection (Figure S1). According to the Rice XPro expression database, the expression of CRCT in the vascular tissues of root isolated by laser

337 microdissection was greatly higher than that in other tissues of root (Figure S2). These findings
338 confirm that the expression of CRCT is basically limited to vascular tissues.
339 In leaf blade, the expressions of *OsGPT2* and *OsBEI* were also predominantly observed in the
340 phloem (Figures 2b, e). The expressions of other genes were detected in both the mesophyll cell
341 and vascular bundles, whereas the expressions of *OsAGPS1* and *OsPho1* in the vascular bundle
342 were lower than those in the mesophyll cell (Figures 2c-e). The cell-specific expression of
343 starch synthesis genes in the leaf sheath was largely similar to that in the leaf blades, although
344 the leaf sheath contained storage parenchyma cells, where the accumulation of starch occurred
345 (Figures 2g-l). In the leaf sheath, *OsGPT2* was expressed in cells other than vascular bundle
346 (Figure 2h). The expression of *OsAGPL1* in the vascular bundle was lower than that in the
347 mesophyll and storage parenchyma cells (Figure 2i). The expression of *OsBEI* was observed in
348 the entire vascular bundle and not limited to the phloem (Figure 2k).
349 The expression levels of these starch synthesis-related genes were also analyzed in other
350 organs (Figure S3, S4 and S5). Both *CRCT* and *OsGPT2* were predominantly expressed in the
351 vascular bundle of the culm (Figure S3). As observed with *CRCT*, the expression of *OsGPT2*
352 and *OsBEI* were highly detected in the non-elongation internode (Figure S3). *OsAGPL1,*
353 *OsAGPS1 and OsPho1* were expressed in anther, although the expression levels were rather low
354 judging from the staining intensities (Figure S5). Unexpectedly, the tissue- and cell- specific
355 expression patterns of *CRCT* was rather similar to those of *OsGPT2* and *OsBEI*, despite there
356 being no correlation between *CRCT* expression level and *OsGPT2* and *OsBEI* expression levels
357 among rice cultivars.
358 The organ-specific expression of starch synthesis-related genes was also analyzed by
359 qRT-PCR (Figure S6). Overall, the starch synthesis-related genes selected in this study were
360 mostly expressed in the vegetative organs such as the leaf blade, leaf sheath and culm, though as
361 an exception, *OsBEI* was also expressed in seed. Among the tested organs, *CRCT* expression
362 was highest in the leaf blade. In contrast, the expression of all other starch synthesis-related
363 genes was highest in the culm. In addition, the expression levels of *OsAGPL1*, *OsAGPS1* and
364 *OsPho1* were higher in the leaf sheath than in the leaf blade. This result is inconsistent with our

365 previous report showing a high level of *CRCT* expression in the leaf sheath (Morita et al., 2015).
366 Previously, the expression of *CRCT* in the leaf sheath was analyzed at the seedling stage, and it
367 was higher than that in the leaf blade. Thus, it is thought that *CRCT* expression in the leaf blade
368 exceeds in the leaf sheath during plant maturation.

369 The expression of *CRCT* in the leaf blade and leaf sheath was further compared during
370 diurnal changes in matured plants in the vegetative stage by qRT-PCR and western blot analyses
371 (Figure 3). As reported previously (Morita et al., 2015), the transcript level of *CRCT* in the leaf
372 blade was higher during the light period than in the dark period as assessed by qRT-PCR. The
373 transcript level of *CRCT* in the leaf sheath was low at the beginning of the light period but then
374 increased and peaked at the end of the light period. Throughout the day, the transcript level of
375 CRCT in the leaf blade was higher than that in the leaf sheath. The protein level of CRCT,
376 however, was barely detectable in the leaf blade (Figure 3b). In the leaf sheath, the CRCT
377 protein was clearly detected and varied in a pattern similar to the transcript level. Thus, in
378 contrast to the transcript level, the protein level of CRCT in the leaf sheath was always higher
379 than that in the leaf blade.

380

381 **3.3 Subcellular localization of CRCT**

382

383 CRCT contains a CCT domain which usually has an NLS. Prediction of the subcellular
384 localization of CRCT by NLS mapper (http://nls-mapper.iab.keio.ac.jp) yielded a moderate
385 score (5.4), suggesting localization to both the nucleus and the cytoplasm and identified putative
386 bipartite NLS within the CCT domain (Figure S7). To clarify the exact subcellular localization
387 of CRCT, the fusion proteins of the full-length CRCT with GFP (FL-CRCT::GFP) and the CCT
388 domain with GFP (CCT::GFP) were expressed in epidermal cells of onion (*Allium cepa*). The
389 GFP fluorescence of FL-CRCT::GFP was observed at the nucleus and outside the nucleus,
390 possibly the cytosol (Figure 4). The GFP fluorescence of nucleus in FL-CRCT::GFP was more
391 predominant than that in GFP alone. In addition, the GFP fluorescence at the nucleus was more
392 specifically detected in CCT::GFP. These findings indicate that the CRCT protein can localize to

393 the nucleus, and the CCT domain of CRCT is involved in the nuclear localization.

394

395 **3.4 Identification of CRCT target genes**

396

397 CRCT contains a CCT domain at the C-terminal region. The CCT domains of CONSTANS and
398 TOC1 were shown to directly bind to CORE elements (TGTG(X_{2-3})ATG) and are involved in
399 the regulation of gene expression (Tiwari et al., 2010; Gendron et al., 2012). To clarify whether
400 CRCT can bind to the 5'-flanking regions of starch synthesis-related genes, ChIP-qPCR was
401 conducted using the FLAG-CRCT overexpression line. Primers for qPCR were designed at
402 300-400 bp intervals on 5'-flanking regions of the starch synthesis-related genes (Figure 5a).
403 The amplicons designed at the position 10 of *OsGPT2*, the position 8 of *OsAGPL1*, and the
404 position 1 of *OsPho1* were enriched over 100 fold in ChIP DNA compared to input DNA
405 (Figure 5b, c, f). Additionally, the amplicons designed at the position 6 of *OsBEI* and the
406 positions 4 to 7 of *OsAGPS1* were enriched several dozen times by ChIP (Figure 5d, e). These
407 results suggest that CRCT can associate with the promoter regions of these genes, especially
408 *OsAGPL1*, *OsGPT2* and *OsPho1 in vivo*. The CORE element was found in 5'-flanking regions
409 (within 5 kb of the translation initiation) of *OsGPT2*, *OsAGPL1*, *OsAGPS1* and *OsBEI* (Figure
410 5a, Table S2). A CORE element was present in the ChIP enriched position 6 of *OsBEI*. However,
411 other positions of amplicons enriched by ChIP do not overlap the CORE elements. Additionally,
412 the 5'-flanking regions of *OsPho1* do not contain a CORE element. Thus, their presence can not
413 explain the results of our ChIP assay. The CCT domain of Ghd7 can bind to more simple DNA
414 elements such as T1ME (CACA) and G-box (CACG) (Nemoto, Nonoue, Yano, & Izawa, 2016).
415 These elements can be found more in the starch synthesis related genes. Thus, it is likely that
416 the CRCT binds to some elements other than the CORE element.

417

418 **3.5 Molecular weight estimation of CRCT**

419

420 Western blot analysis was carried out to detect CRCT in the leaf sheath of CRCT

overexpression line and knockout line (Figure 6a). The expression of CRCT was significantly increased in the CRCT overexpression line. In contrast, the CRCT band was not detected in the CRCT knockout line, which was produced by the CRISPR/Cas9 system.

To estimate the molecular weight of CRCT *in vivo*, gel filtration chromatography was performed using the crude extract prepared from the CRCT overexpression line. CRCT was eluted around fraction 22 (Figure 6b). Based on the relationship between the molecular weights of standard proteins and their fraction numbers, the molecular weight of CRCT was estimated to be 270 kDa (Figure 6c). According to the deduced amino acid sequence of CRCT, a monomer of CRCT is only 34.2 kDa, suggesting that CRCT may form oligomers or stably interact with other proteins.

3.6 CRCT forms a complex with 14-3-3 proteins

To clarify the structural component of the CRCT complex, an immunoprecipitation was carried out using the FLAG-CRCT overexpression line (driven by the *Actin* promoter) and CRCT knockout line. At the beginning of this experiment, both the CRCT antibody and the FLAG antibody were tested, so the knockout mutant was used as the reference instead of the wild type. There were no apparent differences in the band pattern of WT and CRCT knock-out mutant after SDS-PAGE followed by Coomassie blue staining (Figure 6a). The FLAG antibody was used going forward because it was more specific than the CRCT antibody. The FLAG-CRCT fusion protein was detected by immunoblot analysis both in the input and immunoprecipitation with the FLAG antibody (Figure 7). Some silver stain bands (Band 1, 2 and 3) were detected only in the FLAG-CRCT overexpression line and not in CRCT knockout line (Figure 7). MS analysis with MASCOT search indicated that Band 1 contained 60S acidic ribosomal protein and guanine nucleotide-binding protein β. Bands 2 and 3 contained three 14-3-3-like proteins (GF14B, GF14E, GF14F) and two 14-3-3-like proteins (GF14A, GF14C), respectively (Table 1). These five 14-3-3-like proteins showed higher MS scores than the proteins from band 1 and mutually share high amino acid sequence identity (Yao, Du, Jiang, & Liu, 2007). Thus, we

selected GF14B from band 2 and GF14A from band 3 for subsequent analyses of interaction with CRCT.

A yeast two-hybrid analysis was performed to confirm the interactions between CRCT and the 14-3-3 proteins (Figure 8). Full length CRCT and 14-3-3 proteins (GF14A and GF14B) were fused to the GAL4 activation domain and GAL4 DNA binding domain, respectively. The growth of yeast with empty vectors was not observed on the SD^{3-} plate, whereas the growth of yeast with CRCT and 14-3-3 proteins were observed under the condition, indicating that CRCT could interact with both GF14A and GF14B. The 14-3-3 protein binding motif was reported to be (R/K)X_{1-3}(S/T)XP and the S/T in this motif should be phosphorylated to bind to 14-3-3 proteins (Chen et al., 2019). CRCT contains the 14-3-3 binding motif KEKPSVP upstream of the CCT domain (Figure S7 and S8; Table S3). The CCT domain of CRCT and the 14-3-3 proteins were fused to the GAL4 DNA binding domain and GAL4 activation domain, respectively. The growth of yeast with these vectors was not observed in the SD^{3-} plate (Figure S8b), indicating that the CCT domain alone could not interact with the 14-3-3 proteins, and it is likely that the 14-3-3 binding motif found in CRCT is necessary for the interaction between CRCT and 14-3-3 proteins.

The interaction between CRCT and GF14A was further investigated by a bimolecular fluorescence complementation (BiFC) assay (Figure 9). Among GFP variants, the superfolder GFP (sfGFP) was used for this BiFC analysis because sfGFP-based BiFC is the brightest in plants compared with other GFP variants used in BiFC (Fujii, & Kodama, 2015). The N- and C-terminals of sfGFP were fused to the N-terminal ends of CRCT and GF14A and expressed in onion epidermal cells. Fluorescence from the reconstituted sfGFP protein was detected when CRCT and GF14A were coexpressed, and this fluorescence matched with the position of nuclei, as visualized by DAPI staining. The 14-3-3 proteins were previously reported to be present as dimers in the nuclear and non-nuclear compartments other than vacuoles (Bihn et al., 1997). Thus, we used GF14A as a positive control of BiFC. As expected, a significant fluorescent signal was observed in the nuclear and non-nuclear compartments when GF14A fused to both the N- and C-terminal parts of sfGFP were coexpressed. In contrast, sfGFP fluorescence was

quite low when CRCT fused to both the N- and C-terminal parts of sfGFP were coexpressed, suggesting that the oligomerization of CRCT is not likely. In our BiFC analysis, self-assembly of the sfGFP was unlikely because sfGFP fluorescence was quite low when 7-methylxantine methyltransferase (MXMT), an arbitrary cytosolic protein was coexpressed with CRCT. These results indicate that CRCT is mostly in close contact with 14-3-3 proteins in the nucleus.

3.7. Transcriptional activation activity of CRCT

Transcriptional activation activity of CRCT was evaluated using fusions of various length of CRCT with a Gal4 DNA-binding domain in yeast (Figure S9). In this experiment, the growth of yeast in SD^{2-} plate (-Trp, -His) indicates the activation of transcription of reporter gene. Transcriptional activation activity of CRCT was detected at N-terminal region (1-93) and central region (91-234). However, C-terminal region of CRCT (235-308), i.e., CCT domain did not show transcriptional activation activity. These results demonstrate that CRCT should be a transcriptional activator and may have more than one transcriptional activation domains.

4 DISCUSSION

We previously showed that CRCT is a positive regulator of starch synthesis in rice, but the underlying molecular function of CRCT remained elusive. In this study, it was found that CRCT forms a complex with 14-3-3 proteins (Figures 7, 8 and 9; Table 1). Although 14-3-3 proteins are well characterized and play a role in the regulation of metabolism and signal transduction for various developmental processes and biological responses, the physiological significance of this CRCT/14-3-3 complex is unknown.

BiFC analysis suggests that the CRCT/14-3-3 complex should mainly occur in the nucleus (Figure 9). 14-3-3 proteins in plants are observed in various subcellular compartments including the nucleus (Bihn et al., 1997). It is well known that florigen such as rice Heading date 3a forms a complex with transcription factor FD1 and 14-3-3 protein to control flowering related genes in

505 the nucleus (Taoka et al., 2011). In this case, FD1 binds to DNA in the form of a complex, and
506 14-3-3 proteins plays the role of adaptor. Among CCT proteins, CONSTANS was shown to
507 interact with 14-3-3 isoforms by yeast two-hybrid and immunoprecipitation assays (Mayfield,
508 Folta, Paul, & Ferl, 2007). Actually, CONSTANS contains a 14-3-3 binding motif upstream of
509 its CCT domain, just like as CRCT (Table S3). Knockout mutants of 14-3-3 isoforms showed a
510 late flowering phenotype similar to the knockout mutant of CONSTANS (Mayfield, Folta, Paul,
511 & Ferl, 2007), suggesting that the interaction with 14-3-3 proteins are necessary for the proper
512 function of CONSTANS. Thus, it is possible that interactions with 14-3-3 proteins are
513 prerequisite for CRCT to control the expression of starch synthesis-related genes in the nucleus.
514 However, the molecular weight of the complex containing CRCT *in vivo* was estimated to be
515 270 kDa by gel filtration chromatography (Figure 6). The monomers of GF14A and GF14B are
516 estimated to be 29.0 kDa and 29.9 kDa, respectively, based on their amino acid sequences. In
517 general, 14-3-3 proteins forms dimers *in vivo*. According to BiFC analysis, CRCT is possibly
518 present as monomer (Figure 9). As the CRCT monomer is 34.2 kDa, the complex of a CRCT
519 monomer and 14-3-3 dimer should be 92.2-94.0 kDa. This molecular weight is lower than the
520 estimation by gel filtration chromatography. The estimation of molecular mass by gel filtration
521 is affected by the shape of protein complex. Thus, there is a possibility that actual molecular
522 mass of CRCT complex can be smaller than our estimation. As another possibility, there are
523 other interacting factors necessary for CRCT to function that are not yet identified.
524 The up-regulation of CRCT by sugar was reduced by nitrogen treatment (Morita et al., 2015).
525 Considering this C/N response, some functional relation to CRCT can be expected with ATL31,
526 a ubiquitin ligase. In *Arabidopsis*, the stability of the 14-3-3 protein regulated by ALT31
527 determined the resistance to C/N stress (Sato et al., 2011). According to their proposed
528 mechanism, the interaction of 14-3-3 protein may inactivate CRCT. The overexpression of
529 CRCT may lead to increases in the level of unbound free CRCT, which enable the up-regulation
530 of the starch synthesis-related genes. In accordance with this hypothesis, it was reported that the
531 starch content was significantly decreased in the leaves of *Arabidopsis* by the overexpression of
532 14-3-3 proteins (Diaz et al., 2011). Furthermore, antisense knockdown of 14-3-3 proteins

greatly increased the starch accumulation (Sehnke et al. 2001). However, the expression level of 14-3-3 proteins can also affect the activity of key enzymes involved in carbon and nitrogen metabolism (Sehnke et al. 2001, Diaz et al., 2011). Therefore, the contribution of CRCT to starch content in 14-3-3 overexpression line and knockdown line requires more clarification.

The 14-3-3 family comprises eight members in rice (Chen, Li, Sun, & He, 2006; Yao, Du, Jiang, & Liu, 2007). These can be divided into ε-like groups and non-ε groups. Non-ε groups including GF14A and GF14B are highly homologous to each other but show different patterns in organ specific expression and stress response. The expression of *GF14B* was reported to be high in roots and low in reproductive organs, whereas the expression of *GF14A* was low in all organs (Yao, Du, Jiang, & Liu, 2007). According to a rice gene expression database, *GF14A* is actually expressed in most organs at a relatively constant level (Figure S10). Most non-ε 14-3-3 proteins other than *GF14C* were induced by pathogen infection, whereas *GF14C* was markedly induced by abiotic stress such as salinity or drought (Chen, Li, Sun, & He, 2006). These observations suggest that 14-3-3 proteins share functions depending on organs and conditions. Among rice non-ε group 14-3-3 proteins, GF14A and GF14B are divided into different clades (Chen, Li, Sun, & He, 2006), both of which can interact with CRCT (Figure 8). In addition, MS analysis of protein that coimmunoprecipitated with CRCT detected other 14-3-3 proteins such as GF14C, GF14E and GF14F (Table 1). From these observations, it is likely that CRCT can interact with 14-3-3 proteins other than GF14A and GF14B. Therefore, it is difficult to further discuss the significance of the CRCT/14-3-3 complex from the information of 14-3-3 proteins.

In this study, ChIP analyses suggested that all of starch synthesis related genes analyzed can be target genes of CRCT (Figures 5). However, the cell specific expression of these genes analyzed by the promoter *GUS* were clearly different from *CRCT* (Figure 2; Figures S3, S4 and S5). The cell specific expression of *CRCT* was rather similar to that of *OsGPT2* and *OsBEI* (Figure 2; Figures S3, S4 and S5). It was also puzzling that the expression of *CRCT* transcript in the leaf sheath was lower than that in the leaf blade, whereas the protein level of CRCT was higher in the leaf sheath than in the leaf blade (Figure 3). Some mobile transcription factors have been reported in plants. For example, a GRAS transcription factor SHORT-ROOT and

561 homeobox KNOTTED1 proteins were shown to move from one cell to another (Lucas et al.,
562 1995; Wu, & Gallagher, 2014). We hypothesize that CRCT protein may move somehow
563 between cells, and the place where CRCT is expressed may be different from the place where it
564 functions. However, it is also possible that *CRCT* mRNA moves between cells, or the stability
565 of CRCT protein in the leaf blade is lower than that in the leaf sheath. Further study is needed to
566 find out the mechanism.

567 The starch content in the leaf sheath was evidently correlated with the expression level of
568 *CRCT* in the *CRCT* overexpression and knockdown lines (Morita et al. 2015; Morita et al. 2016).
569 Thus, we consider that *CRCT* must be involved in starch accumulation, and may be related to
570 the natural variation of starch content in the leaf sheath of rice (Goda et al., 2016). However, in
571 our previous study, we constitutively overexpressed *CRCT* using *Actin* promoter (Morita et al.,
572 2015). Thus, increased starch content in our overexpression lines may be an effect of ectopic
573 expression. In this study, the difference in the starch content was not correlated with the
574 expression level of *CRCT* among six rice cultivars (Figure 1). Nevertheless, we found a
575 significant correlation between the expression of *CRCT* and starch synthesis-related enzymes
576 (Figure 1). Therefore, we presume that this contradiction could be due to the difference in
577 expression level of *CRCT* between cultivars being smaller than the difference in the expression
578 level in transgenic lines. Although there is an inconsistency in the place of expression, CRCT
579 must be an important factor controlling starch synthesis. Moreover, this study provide important
580 progress towards the understanding of the mechanism of how CRCT controls starch synthesis in
581 rice.
582

583 **ACKNOWLEDGEMENT**

584

585 We thank Dr. Yutaka Kodama (Utsunomiya University) for generous gifts of vectors and
586 technical assistance of BiFC analysis. We thank Dr. Yasuo Niwa (University of Shizuoka,
587 Japan) for a generous gift of vector of GFP analysis. We thank Dr. Masaki Endo (National
588 Agriculture and Food Research Organization) for generous gifts of vectors and technical
589 assistance of CRISPR/Cas9. We thank Dr. Ryoko Kusakabe and Prof. Masaaki Miyamoto (Kobe
590 University) for technical assistance of LC-MS analysis. We thank Dr. Ryu Fujimoto (Kobe
591 university) for technical assistance of ChIP analysis.

592

593 **CONFLICT OF INTEREST**

594

595 The authors declare no conflicts of interest.

596

597 **AUTHOR CONTRIBUTIONS**

598

599 Hiroshi Fukayama and Ryutaro Morita designed the research. Naoki Shibatani, Hirofumi
600 Miyagawa, Aiko Koudou, Hiroshi Fukayama, and Ryutaro Morita performed the experiment
601 with the help from Yasuo Yamauchi, Daisuke Matsuoka, Daisuke Sasayama, Tomoko Hatanaka,
602 and Tetsushi Azuma. Hiroshi Fukayama, Naoki Shibatani, Hirofumi Miyagawa, Aiko Koudou,
603 Ryutaro Morita, and Daisuke Matsuoka analyzed the data. Hiroshi Fukayama supervised the
604 research. Hiroshi Fukayama wrote the manuscript.

605

606 **CONFLICT OF INTEREST**

607

608 The authors declare no conflicts of interest.

609

610 **SUPPORTING INFORMATION**

611

612 Additional Supporting Information may be found in the online version of this article.

613 **Figure S1.** Histochemical analysis of *CRCT* promoter::*GUS* expression in leaf blade and leaf

614 sheath treated with sucrose.

615 **Figure S2.** Expression of *CRCT* in root.

616 **Figure S3.** Histochemical analysis of starch synthesis-related gene promoter::*GUS* expression

617 in culm and non-elongation internodes.

618 **Figure S4.** Histochemical analysis of starch synthesis-related gene promoter::*GUS* expression

619 in root.

620 **Figure S5.** Histochemical analysis of starch synthesis-related gene promoter::*GUS* expression

621 in spikelet and hulled seed.

622 **Figure S6.** Organ specificity of the expression of starch synthesis-related genes by qRT-PCR.

623 **Figure S7.** Deduced amino acid sequence of CRCT.

624 **Figure S8.** Yeast-two-hybrid assay analyzing the interaction of CCT domain of CRCT with

625 14-3-3 proteins.

626 **Figure S9.** Transcriptional activation activity of CRCT.

627 **Figure S10.** Organ specificity of the expression of *GF14A* and *GF14B*.

628 **Table S1.** Primers used in this study.

629 **Table S2.** CORE elements found in the 5'-flanking region of starch synthesis-related genes.

630 **Table S3.** 14-3-3 protein binding motif in CCT proteins.

631

632 **DATA AVAILABILITY STATEMENT**

633

634 The data that support the findings of this study are available from the corresponding author

635 upon reasonable request.

636

637

638 **REFERENCE**

639

640 Ainsworth, E.A., & Long, S.P. (2005). What have we learned from 15 years of free-air CO_2
641 enrichment (FACE)? A meta-analytic review of the responses of photosynthesis, canopy
642 properties and plant production to rising CO_2. *New Phytologist*, 165(2), 351-372.
643 Bihn, E.A., Paul, A.-L., Wang, S.W., Erdos, G.W., & Ferl, R.J. (1997). Localization of 14-3-3
644 proteins in the nuclei of *Arabidopsis* and maize. *Plant Joirnal*, 12(6), 1439-1445.
645 Buzas, D.M., Robertson, M., Finnegan, E.J., & Helliwell, C.A. (2011). Transcription-
646 dependence of histone H3 lysine 27 trimethylation at the Arabidopsis polycomb target gene
647 FLC. *Plant Journal*, 65(6), 872-881.
648 Chen, F., Li, Q., Sun, L., & He, Z. (2006). The rice 14-3-3 gene family and its involvement in
649 responses to biotic and abiotic stress. *DNA Research*, 13(2), 53-63.
650 Chen, Y.S., Ho, T.D., Liu, L., Lee, D.H., Lee, C.H., Chen, Y.R., Lin, S.Y., Lu, C.A., & Yu, S.M.
651 (2019). Sugar starvation-regulated MYBS2 and 14-3-3 protein interactions enhance plant
652 growth, stress tolerance, and grain weight in rice. *Proceedings of the National Academy of*
653 *Sciences*, 116(43), 21925-21935.
654 Chiu, W., Niwa, Y., Zeng, W., Hirano, T., Kobayashi, H., & Sheen, J. (1996). Engineered GFP as
655 a vital reporter in plants. *Current Biology*, 6(3), 325-330.
656 Cockram, J., Thiel, T., Steuernagel, B., Stein, N., Taudien, S., Bailey, P.C., & O'Sullivan, D.M.
657 (2012). Genome dynamics explain the evolution of flowering time CCT domain gene
658 families in the Poaceae. *PLoS One*, 7(9), e45307.
659 Cook, J.H., & Yoshida, S. (1972). Accumulation of 14C-labelled carbohydrate before flowering
660 and its subsequent redistribution and respiration in the rice plant. *Japanese Journal of Crop*
661 *Science*, 41(2), 226-234.
662 Diaz, C., Kusano, M., Sulpice, R., Araki, M., Redestig, H., Saito, K., Stitt, M., & Shin, R.
663 (2011). Determining novel functions of Arabidopsis 14-3-3 proteins in central metabolic
664 processes. *BMC Systems Biology*, 5, 192.
665 Fujii, Y., & Kodama, Y. (2015). In planta comparative analysis of improved green fluorescent

proteins with reference to fluorescence intensity and bimolecular fluorescence complementation ability. *Plant Biotechnology*, 32(1), 81-87.

Fujiwara, S., Wang, L., Han, L., Suh, S.-S., Salomé, P.A., McClung, C.R., & Somers, D.E. (2008). Post-translational regulation of the *Arabidopsis* circadian clock through selective proteolysis and phosphorylation of pseudo-response regulator proteins. *Journal of Biological Chemistry*, 283(34), 23073-23083.

Fukayama, H., Fukuda, T., Masumoto, C., Taniguchi, Y., Sakai, H., Cheng, W., Hasegawa, T., & Miyao, M. (2009). Rice plant response to long term CO_2 enrichment: Gene expression profiling. *Plant Science*, 177(3), 203-210.

Gendron, J.M., Pruneda-Paz, J.L., Doherty, C.J., Gross, A.M., Kang, S.E., & Kay, S.A. (2012). *Arabidopsis* circadian clock protein, TOC1, is a DNA-binding transcription factor. *Proceedings of the National Academy of Sciences*, 109(8), 3167-3172.

Gnesutta, N., Kumimoto, R.W., Swain, S., Chiara, M., Siriwardana, C., Horner, D.S., Holt, B.F., & Mantovani, R. (2017). CONSTANS imparts DNA sequence specificity to the histone fold NF-YB/NF-YC dimer. *Plant Cell*, 29, 1516-1532.

Goda, T., Teramura, H., Suehiro, M., Kanamaru, K., Kawaguchi, H., Ogino, C., Kondo, A., & Yamasaki, M. (2016). Natural variation in the glucose content of dilute sulfuric acid-pretreated rice straw liquid hydrolysates: Implications for bioethanol production. *Bioscience, Biotechnology, and Biochemistry*, 80(5), 863-869.

Kodama, Y., & Wada, M. (2009). Simultaneous visualization of two protein complexes in a single plant cell using multicolor fluorescence complementation analysis. *Plant Molecular Biology*, 70, 211-217.

Li, Y., & Xu, M (2017). CCT family genes in cereal crops: A current overview. *Crop Journal*, 5(6), 449-458.

Lucas, W.J., Bouché-Pillon, S., Jackson, D.P., Nguyen, L., Baker, L., Ding, B., & Hake, S. (1995). Selective Trafficking of KNOTTED1 Homeodomain Protein and Its mRNA Through Plasmodesmata. *Science*, 270(5244), 1980-1983.

Masaki, T., Tsukagoshi, H., Mitsui, N., Nishii, T., Hattori, T., Morikami, A., &

694 Nakamura, K. (2005). Activation tagging of a gene for a protein with novel class of CCT-
695 domain activates expression of a subset of sugar-inducible genes in *Arabidopsis thaliana*.
696 *Plant Journal*, 43(1), 142-152.
697 Masumoto, C., Miyazawa, S., Ohkawa, H., Fukuda, T., Taniguchi, Y., Murayama, S., Kusano,
698 M., Saito, K., Fukayama, H., & Miyao, M. (2010). Phosphoenolpyruvate carboxylase
699 intrinsically located in the chloroplast of rice plays a crucial role in ammonium assimilation.
700 *Proceedings of the National Academy of Sciences*, 107(11), 5226-5231.
701 Matsuoka, D., Yasufuku, T., Furuya, T., & Nanmori, T. (2015). An abscisic acid inducible
702 Arabidopsis MAPKKK, MAPKKK18 regulates leaf senescence via its kinase activity. *Plant*
703 *Molecular Biology*, 87, 565-575.
704 Matsuoka, M., & Numazawa, T. (1991). CIS-acting elements in the pyruvate, orthophosphate
705 dikinase gene from maize. *Molecular and General Genetics*, 228, 143-152.
706 Mayfield, J.D., Folta, K.M., Paul, A.-L., & Ferl, R.J. (2007). The 14-3-3 proteins μ and υ
707 influence transition to flowering and early phytochrome response. *Plant Physiology*, 145,
708 1692-1702.
709 Mikami, M., Toki, S., & Endo, M. (2015). Comparison of CRISPR/Cas9 expression constructs
710 for efficient targeted mutagenesis in rice. *Plant Molecular Biology*, 88, 561-572.
711 Morita, K., Hatanaka, T., Misoo, S., & Fukayama, H. (2014). Unusual small subunit that is not
712 expressed in photosynthetic cells alters the catalytic properties of Rubisco in rice. *Plant*
713 *Physiology*, 164, 69-79.
714 Morita, R., Sugino, M., Hatanaka, T., Misoo, S., & Fukayama, H. (2015). CO_2-Responsive
715 CONSTANS, CONSTANS-Like, and Time of Chlorophyll a/b Binding Protein Expression1
716 Protein is a positive regulator of starch synthesis in vegetative organs of rice. *Plant*
717 *Physiology*, 167, 1321-1331.
718 Morita, R., Inoue, K., Ikeda, K., Hatanaka, T., Misoo, S., & Fukayama, H. (2016). Starch
719 content in leaf sheath controlled by CO_2-Responsive CCT Protein is a potential determinant
720 of photosynthetic capacity in rice. *Plant and Cell Physiology*, 57(11), 2334-2341.
721 Morita, R., Crofts, N., Shibatani, N., Miura, S., Hosaka, Y., Oitome, N.F., Ikeda, K.I., Fujita, N.,

& Fukayama, H. (2019). CO_2-Responsive CCT Protein stimulates the ectopic expression of particular starch biosynthesis-related enzymes, which markedly change the structure of starch in the leaf sheaths of rice. *Plant and Cell Physiology*, 60(5), 961-972.

Morita, S., & Nakano, H. (2011). Nonstructural carbohydrate content in the stem at full heading contributes to high performance of ripening in heat-tolerant rice cultivar Nikomaru. *Crop Science*, 51(2), 818-828.

Nemoto, Y., Nonoue, Y., Yano, M., & Izawa, T. (2016). Hd1, a CONSTANS ortholog in rice, functions as an Ehd1 repressor through interaction with monocot-specific CCT-domain protein Ghd7. *Plant Journal*, 86(3), 221-233.

Okamura, M., Hirose, T., Hashida, Y., Yamagishi, T., Ohsugi, R., & Aoki, N. (2013). Starch reduction in rice stems due to a lack of *OsAGPL1* or *OsAPL3* decreases grain yield under low irradiance during ripening and modifies plant architecture. *Functional Plant Biology*, 40(11), 1137-1146.

Ookawa, T., Yasuda, K., Kato, H., Sakai, M., Seto, M., Sunaga, K., Motobayashi, T., Tojo, S., & Hirasawa, T. (2010). Biomass production and lodging resistance in 'Leaf Star', a new long-culm rice forage cultivar. *Plant Production Science*, 13(1), 58-66.

Robson, F., Costa, M.M.R., Hepworth, S.R., Vizir, I., Pin˜eiro, M., Reeves, P.H., Putterill, J., & Coupland, G. (2001). Functional importance of conserved domains in the flowering-time gene CONSTANS demonstrated by analysis of mutant alleles and transgenic plants. *Plant Journal*, 28(6), 619-631.

Sato, T., Maekawa, S., Yasuda, S., Domeki, Y., Sueyoshi, K., Fujiwara, M., Fukao, Y., Goto, D.B., & Yamaguchi, J. (2011). Identification of 14-3-3 proteins as a target of ATL31 ubiquitin ligase, a regulator of the C/N response in *Arabidopsis*. *Plant Journal*, 68(1), 137-146.

Sehnke, P.C., Chung, H.J., Wu, K., & Ferl, R.J. (2001) Regulation of starch accumulation by granule-associated plant 14-3-3 proteins. *Proceedings of the National Academy of Sciences*, 98(2), 765-770.

Taoka, K., Ohki, I., Tsuji, H., Furuita, K., Hayashi, K., Yanase, T., Yamaguchi, M., Nakashima,

C., Purwestri, Y.A., Tamaki, S., Ogaki, Y., Shimada, C., Nakagawa, A., Kojima, C., & Shimamoto, K. (2011). 14-3-3 proteins act as intracellular receptors for rice Hd3a florigen. *Nature*, 476, 332-335.

Tiwari, S.B., Shen, Y., Chang, H.-C., Hou, Y., Harris, A., Ma, S.F., McPartland,M., Hymus, G.J., Adam, L., Marion, C., Belachew, A., Repetti, P.P., Reuber, T.L., & Ratcliffe, O.J. (2010). The flowering time regulator CONSTANS is recruited to the FLOWERING LOCUS T promoter via a unique cis-element. *New Phytologist*, 187(1), 57-66.

Valverde, F. (2011). CONSTANS and the evolutionary origin of photoperiodic timing of flowering. *Journal of Experimental Botany*, 62(8), 2453-2463.

Wang, Q., Xie, W., Xing, H., Yan, J., Meng, X., Li, X., Fu, X., Xu, J., Lian, X., Yu, S., Xing, Y., & Wang, G. (2015). Genetic architecture of natural variation in rice chlorophyll content revealed by a genome-wide association study. *Molecular Plant*, 8(6), 946-957.

Wu, S., & Gallagher, K.L. (2014). The movement of the non-cell-autonomous transcription factor, SHORT-ROOT relies on the endomembrane system. *Plant Journal*, 80(3), 396-409.

Xu, G., Wang, X., Huang, C., Xu, D., Li, D., Tian, J., Chen, Q., Wang, C., Liang, Y., Wu, Y., Yang, X., & Tian, F. (2017). Complex genetic architecture underlies maize tassel domestication. *New Phytologist*, 214(2), 852-864.

Xue, W., Xing, Y., Weng, X., Zhao, Y., Tang, W., Wang, L., Zhou, H., Yu, S., Xu, C., Li, X., & Zhang, Q. (2008). Natural variation in Ghd7 is an important regulator of heading date and yield potential in rice. *Nature Genetics*, 40, 761-767.

Yao, Y., Du, Y., Jiang, L., & Liu, J.-Y. (2007). Molecular analysis and expression patterns of the 14-3-3 gene family from *Oryza sativa*. *Journal of Biochemistry and Molecular Biology*, 40(3), 349-357.

Yoshinaga, S., Takai, T., Arai-Sano, Y., Ishimaru, T., & Kondo, M (2013). Varietal differences in sink production and grain-filling ability in recently developed high-yielding rice (*Oryza sativa* L.) varieties in Japan. *Field Crops Research*, 150(20), 74-82.

FIGURE LEGENDS

FIGURE 1 Relationship between the expressions of starch synthesis related genes and *CRCT* in the leaf sheath. The 8th leaf sheath at 9.5 leaf stage were harvested at early evening. The expressions of starch synthesis related genes and *CRCT* relative to *Actin* was analyzed by qRT-PCR and expressed as fold relative to the average value of Nipponbare.

FIGURE 2 Histochemical analysis of starch synthesis related gene promoter::*GUS* expression. The transgenic lines were grown for 40 days and its tissues were harvested and stained for 2 days. Cross section of leaf blade (a-f) and leaf sheath (g-l) with *CRCT* (a, g), *OsGPT2* (b, h), *OsAGPL1* (c, i). *OsAGPS1* (d, j). *OsBEI* (e, k) and *OsPho1* (f, l) promoter::*GUS* constructs were observed by light microscope. V, vascular bundle; M, mesophyll cell; S, storage parenchyma cell. Scale bar, 50 μm.

FIGURE 3 Diurnal changes in the expression of CRCT. (a) qRT-PCR analysis of *CRCT*. The expressions of *CRCT* relative to *Actin* are shown. Data represent mean ± SD of four biological replicates. (b) Western blot analysis of CRCT. The soluble proteins were separated by SDS-PAGE and detected by western blot analysis using anti-CRCT antibody. The arrowhead indicates the position of CRCT. In both experiments, the non-transgenic rice plants were grown in the growth chamber of 14 h light (L) and 12 h dark (D) condition. At indicated time, the leaf blade and leaf sheath were collected.

FIGURE 4 Subcellular localization of CRCT. (a) The chimeric constructs used for GFP assay. The full-length *CRCT* or CCT domain of *CRCT* were fused to *GFP*. Black bar indicates the coding region of *CRCT*. White box represents the motifs conserved among some CCT proteins. (b) The fluorescence from GFP. The chimeric constructs were introduced into onion epidermal cells. DAPI was used for staining of nucleus. The fluorescence from GFP and DAPI were observed with a fluorescence microscope at 24 h after transformation. Scale bars, 50 μm.

805

806 **FIGURE 5** ChIP-qPCR analysis of starch synthesis related genes. The 8th leaf sheath at 9.5 leaf
807 stage of FLAG-CRCT expression line was harvested at early evening. ChIP was carried out
808 using anti-FLAG antibodies. Primers used for qPCR were designated at 300-400 bp interval on
809 the 5' flanking region of starch synthesis related genes (a). Amplicons are shown in red bar.
810 Blue arrowheads indicate positions of CORE element. DNA contents of the promoter regions of
811 *OsGPT2* (b), *OsAGPL1* (c), *OsAGPS1* (d), *OsBEI* (e) and *OsPho1* (f) co-immunoprecipitated
812 with anti-FLAG antibody (ChIP) and in input were analyzed by qPCR. Enrichment of DNAs in
813 ChIP relative to input is shown. Data represent mean ± SD of four biological replicates. 18S
814 ribosome RNA gene was used as a reference for qPCR.

815

816 **FIGURE 6** Estimation of molecular weight of CRCT by gel filtration chromatography. (a)
817 Immunoblot analysis of the expression of CRCT in the leaf sheaths of CRCT overexpression
818 line and knockout line. Soluble proteins (4.6 μg) were separated by SDS-PAGE, and detected
819 by Coomassie Blue staining (right panel) or immunoblotting using anti-CRCT antibody (left
820 panel). WT, non-transgenic rice; Ox, CRCT overexpression line; crct, CRCT knockout line. (b)
821 Distribution of CRCT in the fractions of gel filtration chromatography. Soluble proteins from
822 leaf sheath of CRCT overexpression line were separated by gel filtration chromatography using
823 the SMART system with a Superose 12 PC3.2/30 column. Proteins in each fractions were
824 separated by SDS-PAGE, and detected by immuno-blotting using anti-CRCT antibody. CR,
825 recombinant CRCT. (c) Estimation of molecular weight of CRCT. Molecular weight standard
826 proteins, IgM pentamer (1048 kDa), apoferritin (720 kDa), Rubisco (550 kDa), B-phycoerythrin
827 (242 kDa), lactate dehydrogenase (146 kDa), bovine serum albumin (66 kDa) and soybean
828 trypsin inhibitor (20 kDa) were also separated by gel filtration chromatography. Molecular
829 weight of CRCT was estimated to be 270 kDa by a linear regression of molecular weight on
830 fraction number. Molecular weight standard proteins and CRCT are indicated as open circle and
831 closed circle, respectively.

832

FIGURE 7 Immunoprecipitation with FLAG-CRCT. Proteins extracted from the leaf sheathes of CRCT knockout line (crct) and FLAG-CRCT overexpression line (OxFLAG-CRCT) were immunoprecipitated using anti-FLAG antibody (IP). These proteins were separated by SDS-PAGE and detected by immunoblotting using anti-FLAG antibody (left panel) or silver stain (right panel).

FIGURE 8 Yeast two-hybrid assay showing the interaction of CRCT with 14-3-3 proteins. The full-length cDNA of *CRCT* was cloned into the vector containing the *GAL4* activation domain (pAD), and the full length cDNAs of *GF14A* and *GF14B* were cloned into the vector containing the *GAL4* DNA binding domain (pBD). The transformed yeast were grown on SD^{2-} (/–Leu/–Trp) and SD^{3-}(/–Leu/–Trp/–His) plates. The growths of transformed yeast in SD^{2-} and SD^{3-} indicates the transformation of two vectors and the interaction between two proteins, respectively.

FIGURE 9 Interaction of CRCT with GF14A detected by BiFC assay. N-terminal fusion constructs of CRCT and GF14A with N-terminal (GN) and C-terminal (GC) regions of sfGFP were coexpressed in onion epidermal cells after particle bombardment of the chimeric gene constructs. DsRed protein was also coexpressed as a control for the transformation. Fusion constructs of 7-methylxanthine methyltransferase (MXMT) from *Coffea arabica* were used as arbitrary protein control for sfGFP self-assembly. The fluorescence from GFP (green), DsRed (red) and DAPI (blue) was observed with a fluorescence microscope at 24 h after transformation. Scale bars, 50 μm.

TABLE 1 Proteins immunoprecipitated with FLAG-CRCT identified by MS analysis.

RAP-ID[a]	Protein name	Molecular mass (kDa)	MS score[b]
Band 1			
Os08g0130500	60S acidic ribosomal protein P0	34.5	466
Os01g0686800	Guanine nucleotide-binding protein β	36.7	260
Os01g0896700	60S ribosomal protein L5-2	34.8	153
Band 2			
Os04g0462500	14-3-3-like protein GF14B	30.0	906
Os02g0580300	14-3-3-like protein GF14E	29.8	764
Os03g0710800	14-3-3-like protein GF14F	29.3	600
Band 3			
Os08g0480800	14-3-3-like protein GF14A	29.1	606
Os08g0430500	14-3-3-like protein GF14C	29.0	434

Proteins showing MS score higher than 200 are listed.

[a]RAD-ID is the accession number of rice genes in RAP-DB (https://rapdb.dna.affrc.go.jp/).

[b]MS score is the score assigned by MASCOT search.

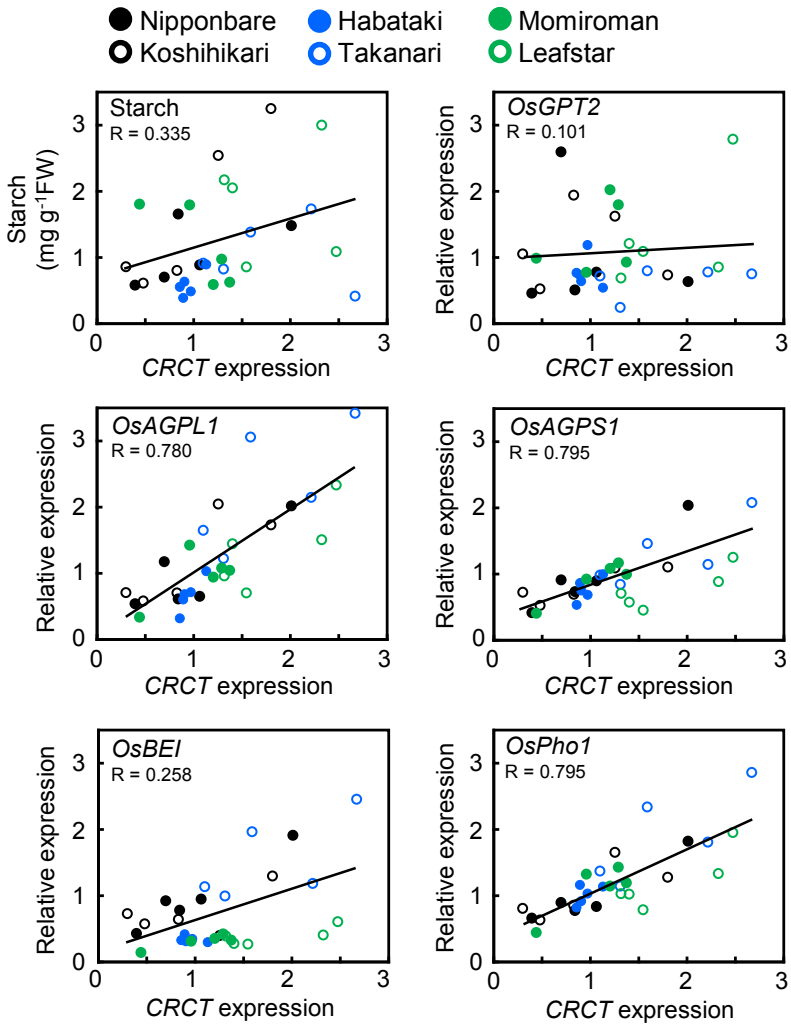

FIGURE 1 Relationship between the expressions of starch synthesis related genes and *CRCT* in the leaf sheath. The 8th leaf sheath at 9.5 leaf stage were harvested at early evening. The expressions of starch synthesis related genes and *CRCT* relative to *Actin* was analyzed by qRT-PCR and expressed as fold relative to the average value of Nipponbare.

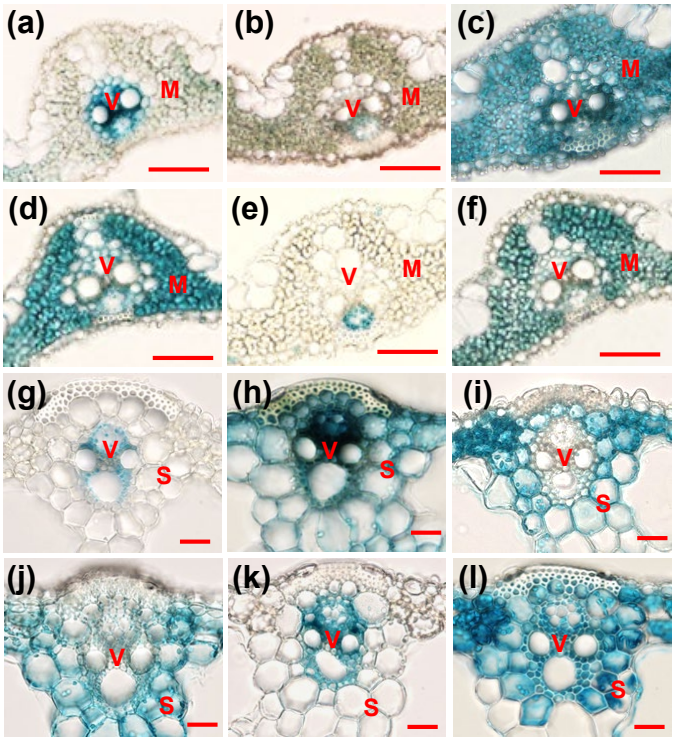

FIGURE 2 Histochemical analysis of starch synthesis related gene promoter::*GUS* expression. The transgenic lines were grown for 40 days and its tissues were harvested and stained for 2 days. Cross section of leaf blade (a-f) and leaf sheath (g-l) with *CRCT* (a, g), *OsGPT2* (b, h), *OsAGPL1* (c, i). *OsAGPS1* (d, j). *OsBEI* (e, k) and *OsPho1* (f, l) promoter::*GUS* constructs were observed by light microscope. V, vascular bundle; M, mesophyll cell; S, storage parenchyma cell. Scale bar, 50 μm.

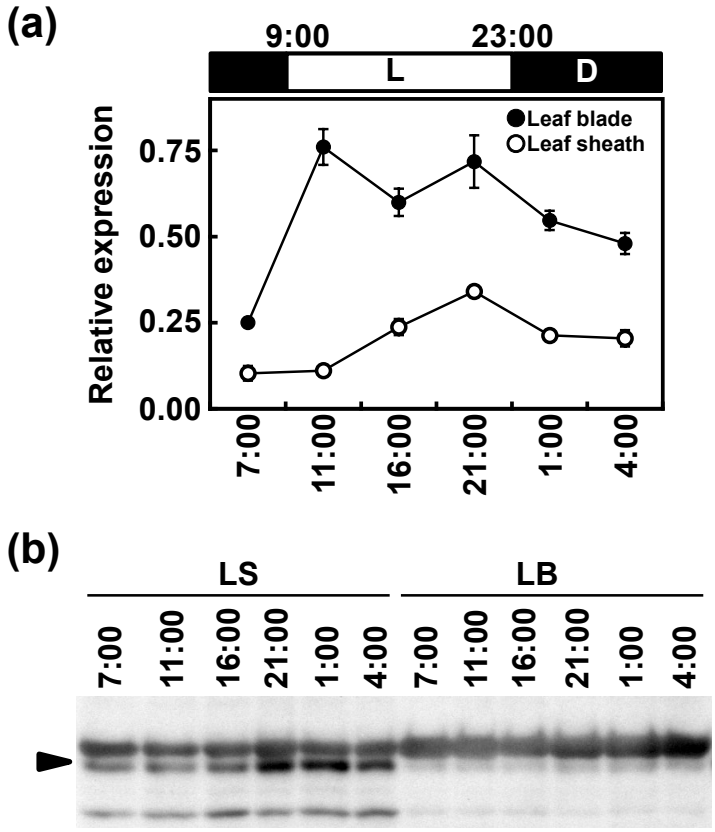

FIGURE 3 Diurnal changes in the expression of CRCT. (a) qRT-PCR analysis of *CRCT*. The expressions of *CRCT* relative to *Actin* are shown. Data represent mean ± SD of four biological replicates. (b) Western blot analysis of CRCT. The soluble proteins were separated by SDS-PAGE and detected by western blot analysis using anti-CRCT antibody. The arrowhead indicates the position of CRCT. In both experiments, the non-transgenic rice plants were grown in the growth chamber of 14 h light (L) and 12 h dark (D) condition. At indicated time, the leaf blade and leaf sheath were collected.

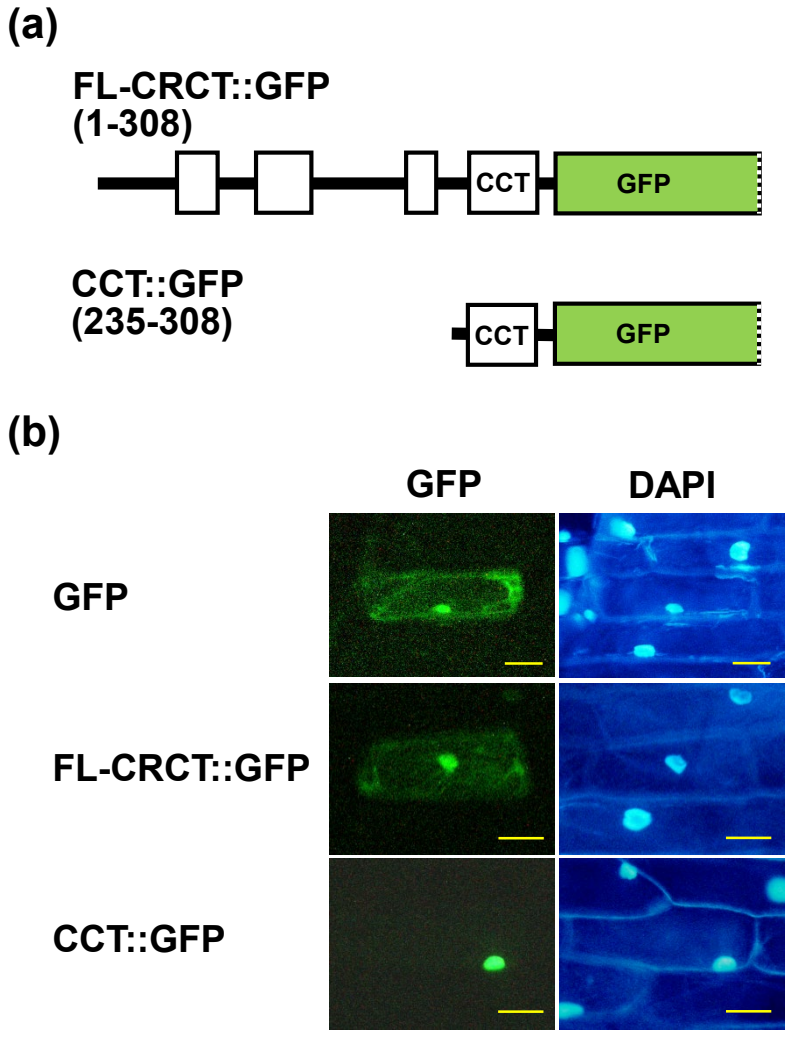

FIGURE 4 Subcellular localization of CRCT. (a) The chimeric constructs used for GFP assay. The full-length *CRCT* or CCT domain of *CRCT* were fused to *GFP*. Black bar indicates the coding region of *CRCT*. White box represents the motifs conserved among some CCT proteins. (b) The fluorescence from GFP. The chimeric constructs were introduced into onion epidermal cells. DAPI was used for staining of nucleus. The fluorescence from GFP and DAPI were observed with a fluorescence microscope at 24 h after transformation. Scale bars, 50 μm.

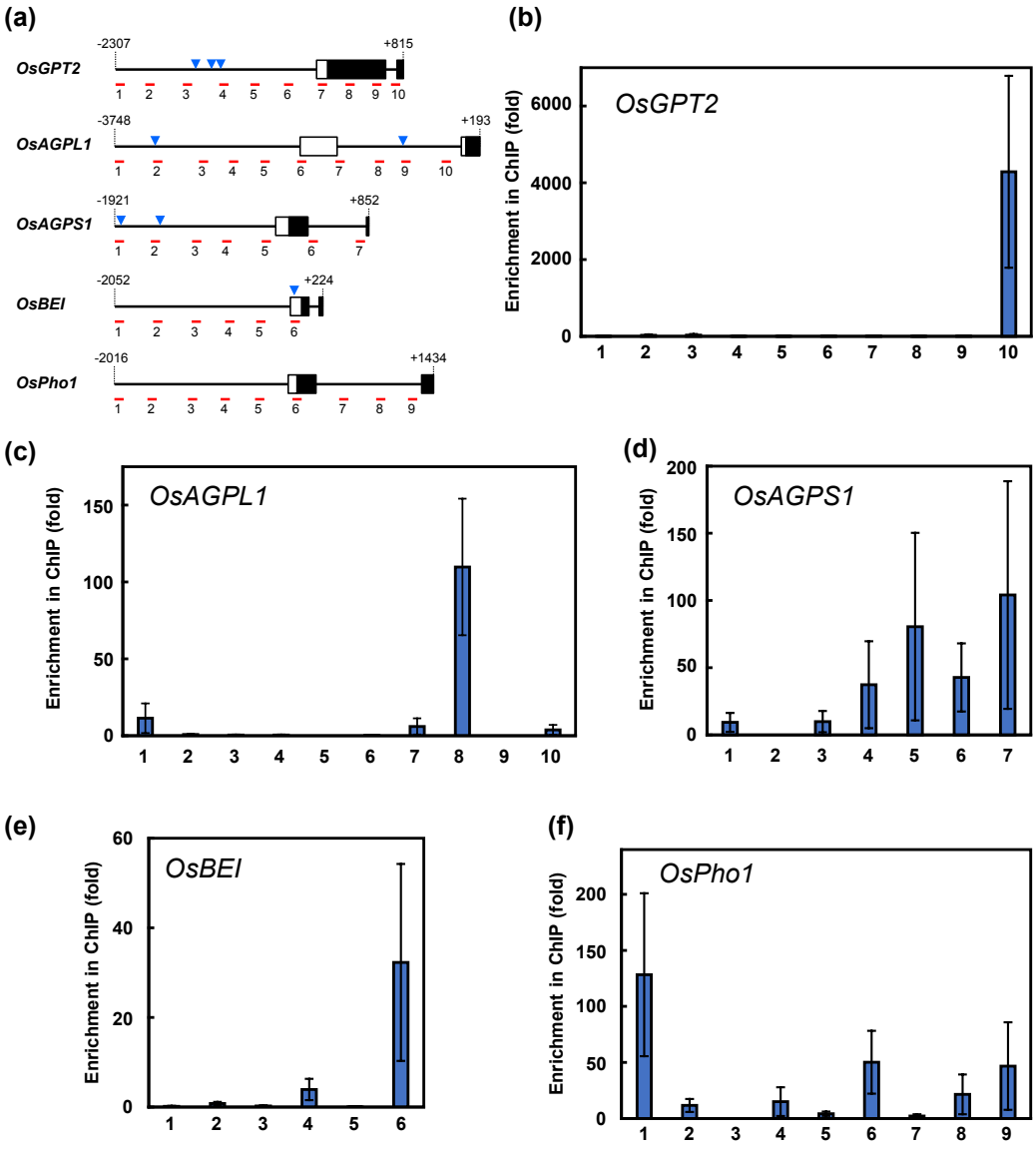

FIGURE 5 ChIP-qPCR analysis of starch synthesis related genes. The 8th leaf sheath at 9.5 leaf stage of FLAG-CRCT expression line was harvested at early evening. ChIP was carried out using anti-FLAG antibodies. Primers used for qPCR were designated at 300-400 bp interval on the 5' flanking region of starch synthesis related genes (a). Amplicons are shown in red bar. Blue arrowheads indicate positions of CORE element. DNA contents of the promoter regions of *OsGPT2* (b), *OsAGPL1* (c), *OsAGPS1* (d), *OsBEI* (e) and *OsPho1* (f) co-immunoprecipitated with anti-FLAG antibody (ChIP) and in input were analyzed by qPCR. Enrichment of DNAs in ChIP relative to input is shown. Data represent mean ± SD of four biological replicates. 18S ribosome RNA gene was used as a reference for qPCR.

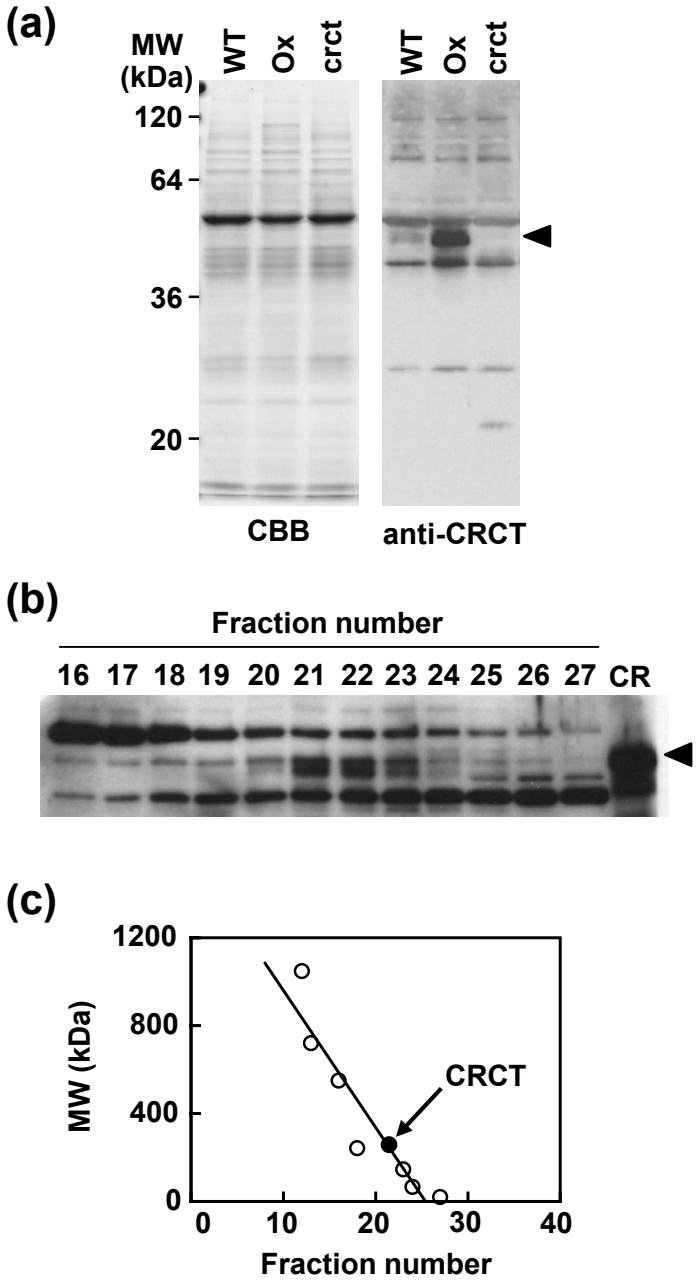

FIGURE 6 Estimation of molecular weight of CRCT by gel filtration chromatography. (a) Immunoblot analysis of the expression of CRCT in the leaf sheaths of CRCT overexpression line and knockout line. Soluble proteins (4.6 μg) were separated by SDS-PAGE, and detected by Coomassie Blue staining (right panel) or immunoblotting using anti-CRCT antibody (left panel). WT, non-transgenic rice; Ox, CRCT overexpression line; crct, CRCT knockout line. (b) Distribution of CRCT in the fractions of gel filtration chromatography. Soluble proteins from leaf sheath of CRCT overexpression line were separated by gel filtration chromatography using the SMART system with a Superose 12 PC3.2/30 column. Proteins in each fractions were separated by SDS-PAGE, and detected by immuno-blotting using anti-CRCT antibody. CR, recombinant CRCT. (c) Estimation of molecular weight of CRCT. Molecular weight standard proteins, IgM pentamer (1048 kDa), apoferritin (720 kDa), Rubisco (550 kDa), B-phycoerythrin (242 kDa), lactate dehydrogenase (146 kDa), bovine serum albumin (66 kDa) and soybean trypsin inhibitor (20 kDa) were also separated by gel filtration chromatography. Molecular weight of CRCT was estimated to be 270 kDa by a linear regression of molecular weight on fraction number. Molecular weight standard proteins and CRCT are indicated as open circle and closed circle, respectively.

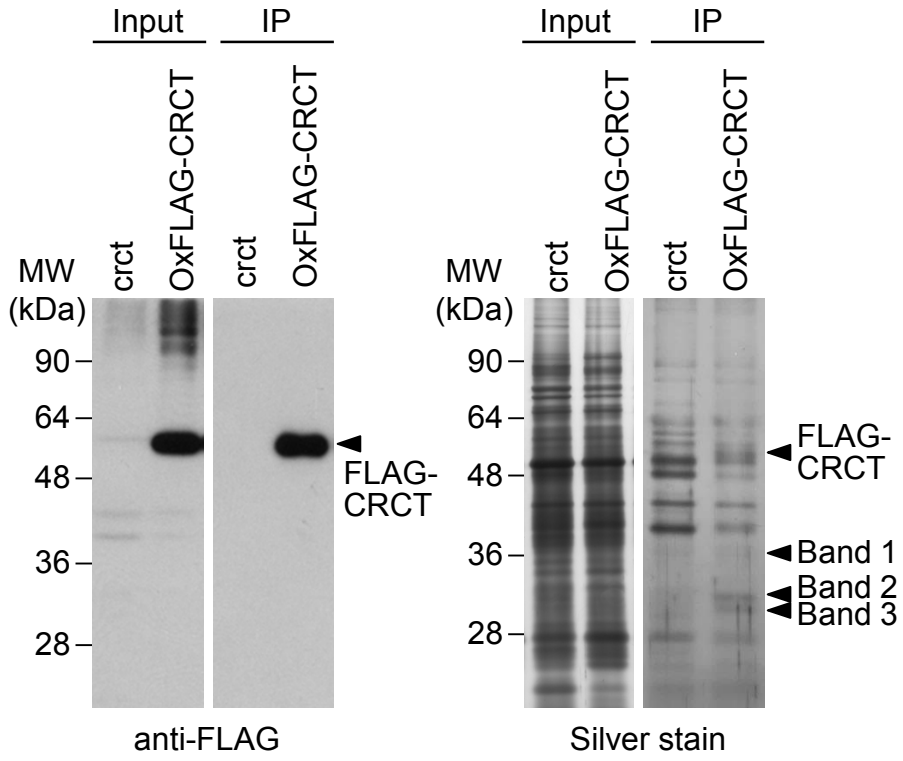

FIGURE 7 Immunoprecipitation with FLAG-CRCT. Proteins extracted from the leaf sheathes of CRCT knockout line (crct) and FLAG-CRCT overexpression line (OxFLAG-CRCT) were immunoprecipitated using anti-FLAG antibody (IP). These proteins were separated by SDS-PAGE and detected by immunoblotting using anti-FLAG antibody (left panel) or silver stain (right panel).

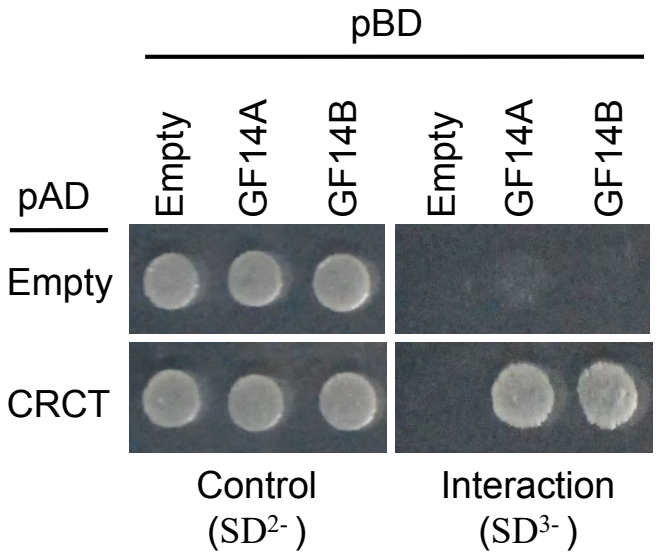

FIGURE 8 Yeast two-hybrid assay showing the interaction of CRCT with 14-3-3 proteins. The full-length cDNA of *CRCT* was cloned into the vector containing the *GAL4* activation domain (pAD), and the full length cDNAs of *GF14A* and *GF14B* were cloned into the vector containing the *GAL4* DNA binding domain (pBD). The transformed yeast were grown on SD^{2-} (/–Leu/–Trp) and SD^{3-}(/–Leu/–Trp/–His) plates. The growths of transformed yeast in SD^{2-} and SD^{3-} indicates the transformation of two vectors and the interaction between two proteins, respectively.

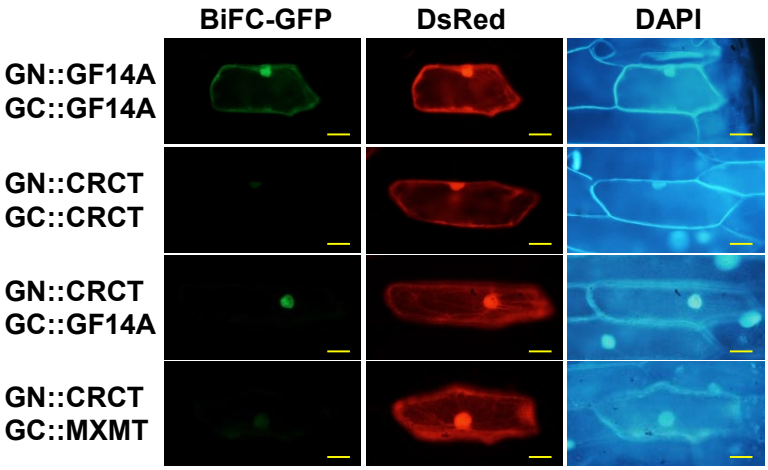

FIGURE 9 Interaction of CRCT with GF14A detected by BiFC assay. N-terminal fusion constructs of CRCT and GF14A with N-terminal (GN) and C-terminal (GC) regions of sfGFP were coexpressed in onion epidermal cells after particle bombardment of the chimeric gene constructs. DsRed protein was also coexpressed as a control for the transformation. Fusion construct of 7-methylxanthine methyltransferase (MXMT) from *Coffea arabica* was used as arbitrary cytosolic protein control for sfGFP self-assembly (Kodama and Wada, 2009). The fluorescence from GFP (green), DsRed (red) and DAPI (blue) was observed with a fluorescence microscope at 24 h after transformation. Scale bars, 50 μm.